CHINESE JOURNAL OF PHYSICS VOL. 52, NO. 2 April 2014

The Local Order and Structural Study of Liquid PdAg Alloy during Cooling Processes under Different Pressures

Sefa Kazanc[1,*] and Fatih Ahmet Celik[2]

[1]*Firat University, Faculty of Education, Physics Teaching Programme, 23119 Elazig, Turkey*
[2]*Bitlis Eren University, Faculty of Arts & Sciences, Physics Department, 13000 Bitlis, Turkey*

(Received November 20, 2012)

The pressure effect on the rapid solidification of a liquid PdAg alloy system is studied by using the molecular dynamics (MD) simulation method. The physical interactions between the atoms in the model alloy systems were modeled using the Sutton-Chen version of the embedded atom method. Crystal and amorphous phase transitions for different pressures were formed at cooling rates of 2×10^{11}, 2×10^{12}, and 2×10^{13} K/s, respectively. The temperatures of crystallization formation at slow cooling rate and the icosahedral order in the amorphous phase at high cooling rate are determined by using a radial distribution function, Wendt-Abraham parameters, and a bond orientational order parameter under different pressures. It is observed that an increase of pressure causes an increase of the crystal and glass formation temperatures.

DOI: 10.6122/CJP.52.852 PACS numbers: 64.70.pm, 61.20.Ja, 34.20.Cf

I. INTRODUCTION

Bulk metallic glasses formed by rapid cooling of liquid alloys are fascinating materials because of their unique physical and mechanical properties. The understanding of the structure and thermal stability of these metastable materials is of great importance from both the fundamental and practical points of view [1–6].

A difficulty of observing a glass transition has been the very high cooling rates, up to 10^6 K/s. To avoid nucleation and the growth of a crystalline phase, one of the typical methods is to keep a high cooling rate, in the range of 10^6–10^{12} K/s. However, due to the demand of a high cooling rate, the rapid solidification method is restricted in most experimental cases [7–10]. Also, it is difficult to study the pressure effect on the glass transition experimentally, because the quenched liquid has a poor thermal stability against crystallization.

Pd-Ag alloys are used as catalysts and their surfaces present many interesting technological characteristics. Recently, interest in Pd-Ag alloys has greatly increased with applications in domains such as dentistry, LCD screens, and hydrogen separation and storage [11].

*Electronic address: skazanc@firat.edu.tr

 © 2014 THE PHYSICAL SOCIETY OF THE REPUBLIC OF CHINA

Atomic simulation techniques have become a powerful tool as they provide physical insight in understanding various phenomena on the atomic scale. Molecular dynamic (MD) simulations are used extensively to investigate the structural or thermodynamic properties of high technological materials, such as intermetallic alloys, semiconductors, polymers, or liquids on the atomic scale [12, 13]. Recently, MD methods have been used for investigating the pressure effect on the rapid solidification structure from the liquid phase [14–17]. Also, in the studies of atomic local order and cluster properties, molecular dynamics (MD) simulations have proved to be one of the most effective approaches, especially in the numerical investigation of the structural evolution of local order. Moreover, in MD simulation studies, the calculation of the bond orientational order parameters has also been a useful method for determining the local symmetric properties of clusters in different phases.

The MD technique consists of the numerical solution of the equations of motion for a system of N atoms [18, 19]. The consistency of the results obtained from the MD simulations with the experimental values depends tightly on the potential energy functions, which are used to model the relevant system. On the other hand, the determination of the potential parameters, especially for the cross potential functions in alloy systems, is still a problem [12, 13]. One of the most useful potential energy methods is the embedded atom method (EAM) based on the many-body interactions proposed by Daw and Baskes [20]. However, due to the simplicity of their potential functions, the versions of the EAM proposed by Vother-Chen [21], Finnis-Sinclair [22], and Sutton-Chen (SC) [23] are widely used to investigate metallic systems and their alloys [24, 25]. Although the first principles methods are the most rigorous, they are limited to very small systems and need computers with higher speed [26].

In the present work, the MD method proposed by Parrinello and Rahman for the NPT ensemble is used to determine the pressure effect on the rapid solidification of a liquid PdAg binary alloy system. To model the interactions between atoms the Sutton-Chen type of embedded atom method based on many-body interaction was used. The liquid phase of the PdAg alloy has been produced and solidified by applying the rapid quenching techniques under 0, 1, and 3 GPa pressure values. The crystallization and glass forming temperatures for model alloy system were obtained. The glass formation tendency and crystallization of liquid Pd–Ag binary alloys was investigated by analyzing the radial distribution function (RDF), volume, and bond orientational order parameter. Pd–Ag alloys show a glass structure at fast cooling rates, while it crystallizes at slow cooling rates.

II. POTENTIAL ENERGY FUNCTION

In this study, to model the physical interactions among the atoms of a binary alloy system, the Sutton-Chen version of the EAM (SCEAM) was used. In a binary alloy of type-a and type-b atoms, the total energy of a crystal with N atoms in the SCEAM methodology

is given by

$$E_T^{SC} = \left\{ \frac{1}{2} \sum_{i^a,j^a}^{N^a} \varepsilon_a \left(\frac{A_a}{r_{ij}} \right)^{n_a} - \sum_{i^a}^{N^a} \varepsilon_a c_a \left[\sum_j \left(\frac{A_{aj}}{r_{ij}} \right)^{m_{ab}} \right]^{1/2} \right\} + \left\{ \frac{1}{2} \sum_{i^b,j^b}^{N^b} \varepsilon_b \left(\frac{A_b}{r_{ij}} \right)^{n_b} - \sum_{i^b}^{N^b} \varepsilon_b c_b \left[\sum_j \left(\frac{A_{bj}}{r_{ij}} \right)^{m_{ba}} \right]^{1/2} \right\} + \frac{1}{2} \sum_{i^a,j^b}^{N^{ab}} \varepsilon_{ab} \left(\frac{A_{ab}}{r_{ij}} \right)^{n_{ab}} + \frac{1}{2} \sum_{i^b,j^a}^{N^{ba}} \varepsilon_{ba} \left(\frac{A_{ba}}{r_{ij}} \right)^{n_{ba}}, \quad (1)$$

where i^a and i^b indicate summation over type-a and type-b atoms, respectively. The potential parameters for the different types of atoms in an alloy system can be calculated from Lorentz-Berthelet [12]:

$$A_{ab} = A_{ba} = \frac{A_a + A_b}{2}, \quad n_{ab} = n_{ba} = \frac{n_a + n_b}{2}, \quad m_{ab} = m_{ba} = \frac{m_a + m_b}{2}, \quad (2)$$

$$\varepsilon_{ab} = \varepsilon_{ba} = \sqrt{\varepsilon_a \varepsilon_b}. \quad (3)$$

Here A is a parameter with the dimensions of length; m and n are positive integers.

The potential parameters for Pd-Pd, Ag-Ag, and Pd-Ag atomic interactions have been given in Table I according to Ref. [27].

TABLE I: The Sutton-Chen EAM potential parameters for PdAg model alloy system [27].

Interaction	A (Å)	ε (eV)	n	m	c
Pd-Pd	3.89	4.1260×10^{-3}	12	7	108.526
Ag-Ag	4.09	2.5330×10^{-3}	12	6	145.658

III. SIMULATION AND APPLICATION PROCESS

In the MD method used here, both the size and the shape of the MD cell are variable. More detailed expositions of the MD simulation method can be found from the literature [28]. The simulations were performed with the system consisting of 10976 atoms in a cubic box with periodic boundary conditions along all the three directions. The fcc structure for the Pd-20%Ag model alloy systems has been chosen as the starting configuration for the MD computer simulation. The 2195 Ag atoms were randomly assigned on the fcc lattice point. The potential functions were truncated at a cut off distance of $2.2A_{\mathrm{PdPd}}$. The

temperature of the system has been controlled by rescaling the atomic velocities at every two integration steps. The equation of motion is numerically integrated by Gears' 5th order predictor-corrector algorithm. The molecular dynamics time step was set up as 8.03 fs.

The model alloy system is run for 50000 MD step at 2000 K to guarantee an equilibrium liquid phase to obtain the initial configuration for the cooling process. When the model system has reached a stable liquid phase at 0 GPa, it is then cooled from 2000 to 300 K with different cooling rates such as 2×10^{11}, 2×10^{12}, and 2×10^{13} K/s. This process was also carried out for different pressure values such as 1 and 3 GPa.

The bond orientational order parameter is adopted to determine the local symmetry of the clusters [29, 30]. Q_6 is the most important of parameters to detect an icosahedral order in supercooled materials under the high cooling conditions, and, in particular, since the values of Q_6 are sensitive to crystallization under the slow cooling [31], the values of this parameter have increased significantly, indicating the order of the crystalline phase [32].

IV. RESULTS AND DISCUSSION

We analyze the radial distribution function $g(r)$, to investigate the structural properties during the cooling process. Fig. 1 demonstrates the RDF curves at a cooling rate of 2×10^{11} K/s under 0, 1, and 3 GPa pressure values for the binary model alloy system. The model structure is in the liquid phase for all pressure values at 2000 K. However, the RDF shows a crystal structure for all pressure values at the cooling rate of 2×10^{11} K/s and 300 K. A splitting can be seen in the second peak of the RDF at the 1000 K for 0 GPa and at 1100 K for 1 and 3 GPa. This splitting is a characteristic of a metallic glass [33]. As seen from Fig. 1, this glass structure is not stable for all pressure values. As the temperature decreased all the RDF peaks become sharper. The solidification process of the metal begins with nucleation in the liquid, and then develops with nucleus growth [34]. The order degree of the system is strengthened as the crystallization begins [35], and finally a crystalline structure is well represented. At 1000 K, an amorphous like structure appears for 0 GPa pressure value, while crystal structures are clearly seen for 1 and 3 GPa. As seen from Fig. 1, at 300 K and 0 GPa the first and second peaks of the RDF are at the location of 2.77 and 3.95 Å, respectively. The position of the second peak of the RDF indicates the lattice parameter of the PdAg alloy system and its literature value of 3.92 Å [36].

Fig. 2 shows the variation of the volume of the PdAg model alloy system as a function of temperature at the cooling rate of 2×10^{11} K/s for all pressure values. A sudden decrease in volume during the cooling process is due to the liquid to crystal transition [33, 35]. It can be seen from Fig. 2 that the crystallization temperature of the model alloy system is 950 ± 50 K for 0 GPa. However, this temperature is the same, 1050 ± 50 K, for 1 and 3 GPa pressure values. The transition temperature from the liquid phase to the crystal phase increases with increasing pressure. High pressure causes an increase in the density and shortens the distance between atoms. Hence the high pressure is in favour of the formation of the crystal structure [35].

It is known that the local bond orientational order parameter is an important parame-

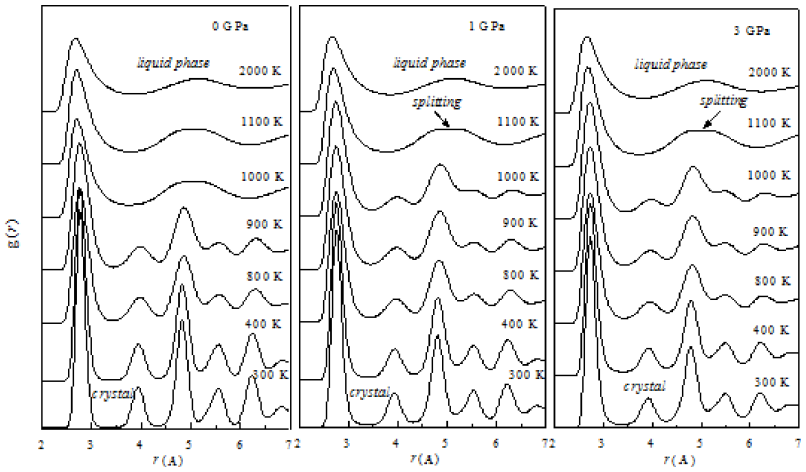

FIG. 1: RDF under different pressures at 2×10^{11} K/s for the PdAg binary alloy system.

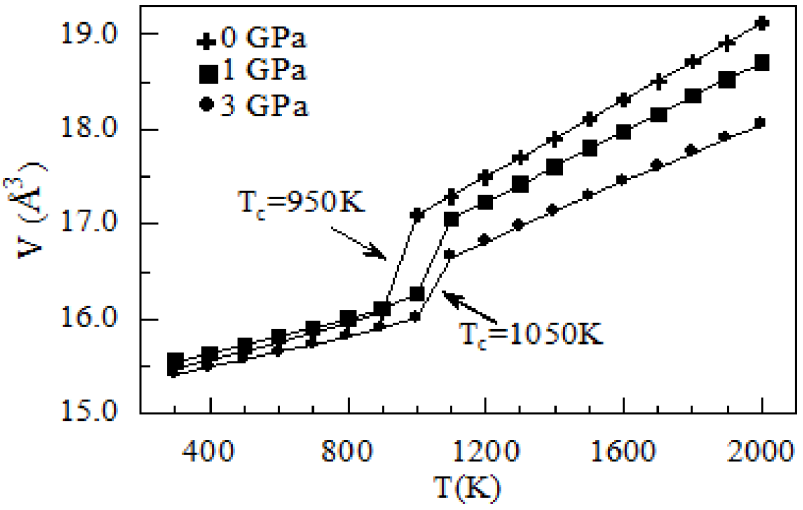

FIG. 2: The variation of volume with temperature of the PdAg alloy system for different pressure values at 2×10^{11} K/s cooling rate.

ter for detecting the crystalline and icosahedral order, the value of Q_6 is a sensitive measure of the different orientational symmetries [37]. The variation of Q_6 against temperature at 0 and 3 GPa pressure values for the cooling rate of 2×10^{11} K/s is given in Fig. 3. The values of the crystallization formation temperatures at 0 GPa and 3 GPa pressures are obtained at about 950 K and 1050 K, respectively. After these temperatures, the value of the bond order parameter gradually saturates with decreasing temperature due to the formation of the crystal phase.

Fig. 4 demonstrates the RDF curves at a cooling rate of 2×10^{12} K/s under different pressure values for the PdAg binary alloy system. The model alloy system is in the liquid

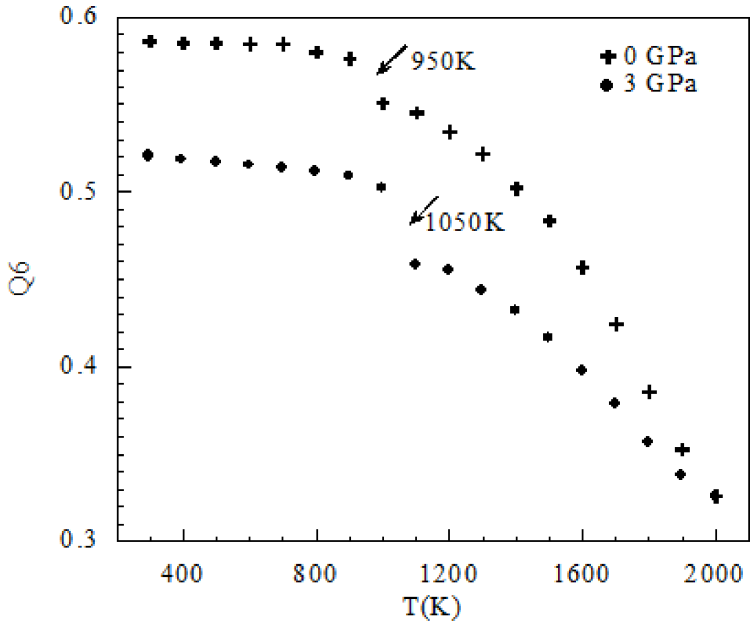

FIG. 3: The value of the bond orientational order parameter under 0 GPa and 3 GPa pressures for the 2×10^{11} K/s cooling rate.

phase for all pressure values at the 2000 K temperature. Cooling to 1400 K, we still observe the structure of a liquid, in fact a supercooled liquid. A splitting can be seen in the second peak of the RDF at 900 K for 0 GPa and at 1000 K for 1 and 3 GPa. This splitting of the second peak is a well-known characteristic feature in RDF of the existence of a metallic glass [33]. As seen from Fig. 4, this glass structure is not stable for all pressure values. A shoulder appears clearly between the first and second peaks at 600 K for 1 GPa and at 800 K for 3 GPa, due to the nucleation of the crystal phase in the amorphous matrix. On the other hand, the amorphous structure at 600 K for 0 pressure value still has thermal stability. When the temperature decreases to 500 K, a shoulder appears between the first and second peaks for 0 GPa. The peaks in the RDF become sharper with a decrease of the temperature of the binary alloy system for all pressure values.

Fig. 5 gives the relationship between the volume and temperature for all pressure values at the 2×10^{12} K/s cooling rate. The crystal transition temperature for binary alloy systems can be determined by the temperature at which the slope of the volume curve changes. At 0 and 1 GPa pressure values, the crystallization temperatures are 550 K and 650 K; at 3 GPa pressure value, the crystallization temperature becomes 850 K.

The variation of Q_6 against temperature at 0 and 3 GPa pressure values for the cooling rate of 2×10^{12} K/s is given in Fig. 6. The values of the crystallization formation temperatures at 0 GPa and 3 GPa pressures are obtained at about 600 K and 800 K, respectively. These results demonstrate that the temperature of the crystallization formation increases with increasing the pressure at slow cooling rates, which is in agreement with

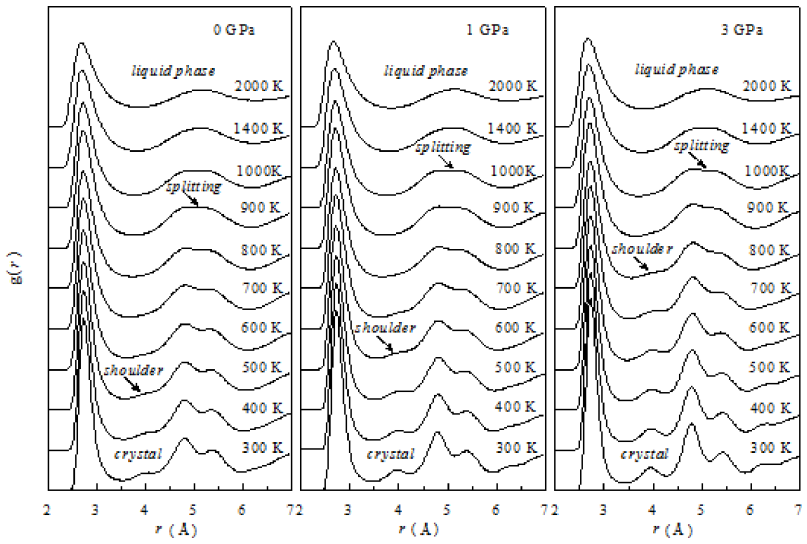

FIG. 4: RDF curves under different pressures at the cooling rate 2×10^{12} K/s.

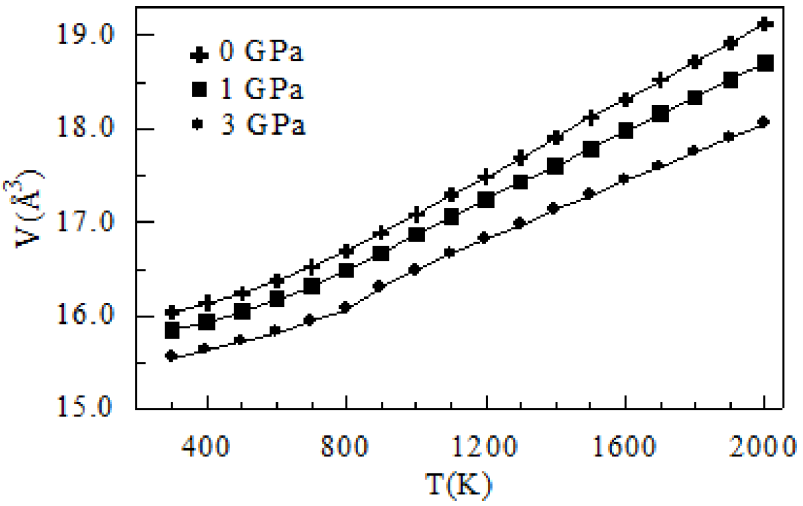

FIG. 5: The variation of the volume with the temperature of the PdAg binary alloy for different pressure values for 2×10^{12} K/s.

Fig. 5.

The variation with temperature of the RDF for the PdAg alloy system at a cooling rate of 2×10^{13} K/s at 0 GPa is given in Fig. 7. The model structure is in the liquid phase at the 2000 K temperature. Cooling to 1100 K, we still observe the structure of a liquid, in fact a supercooled liquid, while the model alloy system is in an amorphous state during the cooling process. A splitting can be seen in the second peak of the RDF at 800 K. This splitting is a characteristic of a metallic glass [33]. Then, as the temperature decreased

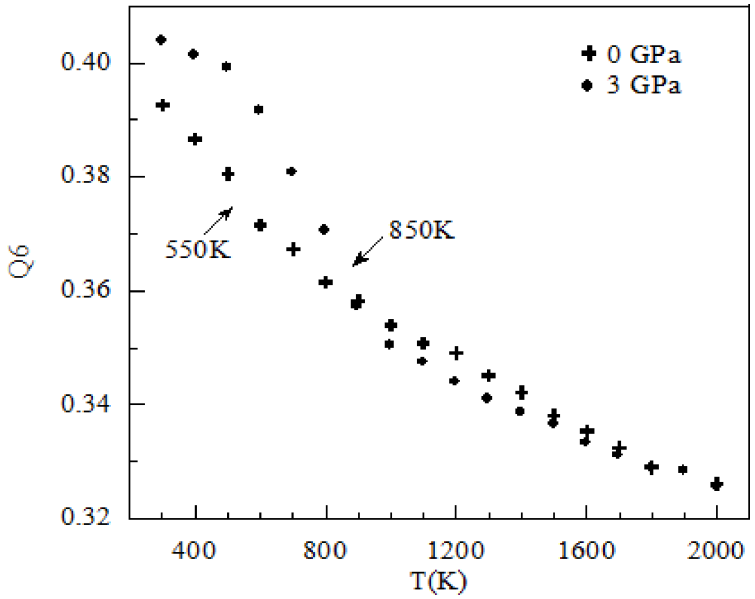

FIG. 6: The value of the bond orientational order parameter under 0 GPa and 3 GPa pressures for the 2×10^{12} K/s cooling rate.

the splitting become sharper. It is seen that, at this cooling rate, an amorphous structure is formed for all pressure values at 300 K. The intensities of the first peak of the RDF curves increase with decreasing temperature, so it can be said that the nearest neighbour coordination is raised during solidification of PdAg binary alloy systems.

The temperature dependence of the Wendt Abraham parameter is a sensitive measure of the glass transition. To define the glass transition temperature in MD simulations, the Wendt–Abraham parameter defined by $g_{\min}/g_{\max}$ is used [38]. Here $g_{\min}$ is the first minimum value and $g_{\max}$ is the first maximum value of the RDF curve.

The formation of a glass leads to a change in the slope, and the intersection of two straight lines yields T_g. Fig. 8 gives the relationship between $g_{\min}/g_{\max}$ and the temperature for all pressure values at the 2×10^{13} cooling rate. There exist two lines with different slopes for all pressure values in Fig. 8. T_g is taken to be the temperature at which these lines intersect with each other, as shown in Fig. 9 plotted for 0 GPa. It is determined from Fig. 8 that the glass forming temperature of the PdAg alloy system for the 2×10^{13} K/s cooling rate under the pressure values of 0, 1, and 3 GPa are 780 K, 820 K, and 890 K, respectively. As seen from the figure, the increase of the pressure and cooling rates increases the glass transition temperature.

From the study performed on Pb [14] and Se [17] matter, it was determined that the glass forming temperature was increased with applied pressure. Under high pressure, the liquid atoms compress each other, causing a much higher density and a smaller amount of free volume. As a result, the decrease in the moving space for particles due to high pressure increases the T_g value [17]. Also, the glassing forming temperature increases with increasing

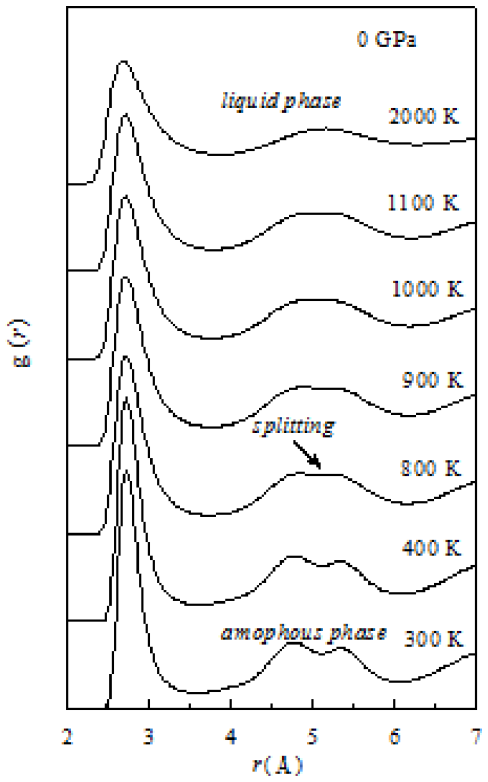

FIG. 7: The RDF curves for 2×10^{13} K/s cooling rate and 0 GPa pressure value.

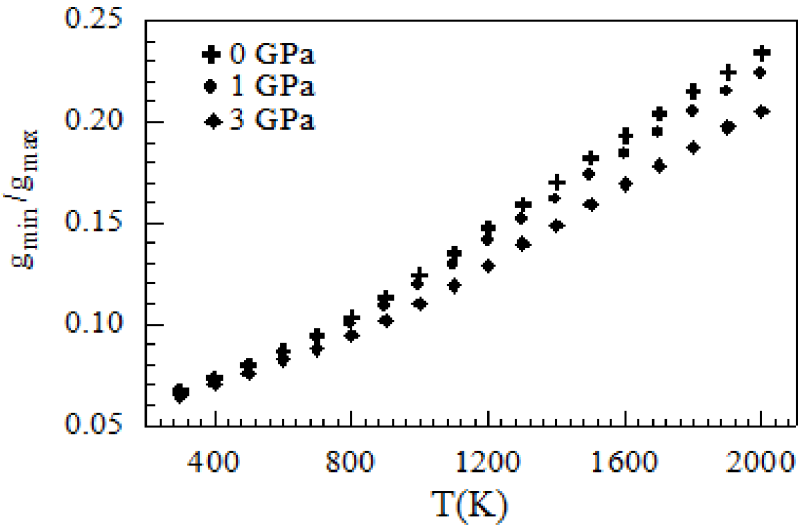

FIG. 8: The glass transition temperature under different pressure values and the 2×10^{13} K/s cooling rate.

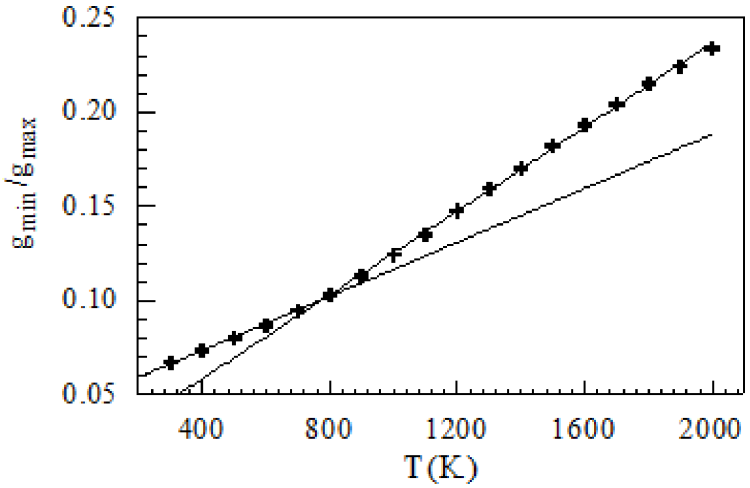

FIG. 9: $g_{\min}/g_{\max}$ is fitted to a linear function to estimate the glass temperature at the 2×10^{13} K/s cooling rate and at the 0 GPa pressure value.

cooling rates. Slower cooling rates allow a greater amount of molecular relaxation to occur in the liquid phase before the structure is frozen at T_g, hence the glass forms at a lower temperature [39].

The bond order parameter of Q_6 can describe the bond order symmetries in the different phases. Especially, the value of the Q_6 parameter in the amorphous phase is a sensitive indicator of icosahedral order. The values of the Q_6 parameter increase with decreasing temperature under 0 and 3 GPa pressures for the 2×10^{13} K/s cooling rate, as seen in Fig. 10. This result shows that the degree of icosahedral order is increased with decreasing temperature under a quick cooling condition. This result is very consistent with the ideas of Hoare [40]. For an ideal icosahedral cluster, the value of Q_6 is 0.6633 [29]. Our simulation results show that the value of the Q_6 does not reach its ideal value at low temperatures, because the structure is not all icosahedral structures; also there are other non-crystalline structures and defective icosahedral clusters. On the other hand, we also find that high pressure has a much more strong effect on the bond orientational order under a high cooling rate, and the icosahedral order increases with increasing pressure; these results are in agreement with other studies, as discussed in [41, 42].

V. CONCLUSION

The evaluation of the crystal order and glass formation at different cooling rates under the various pressures is studied by using a molecular dynamics method proposed by Parrinello-Rahman. The bond orientational order parameter has also been calculated at slow and high cooling conditions in order to detect the crystalline and icosahedral order. The results reached can be summarised as follows:

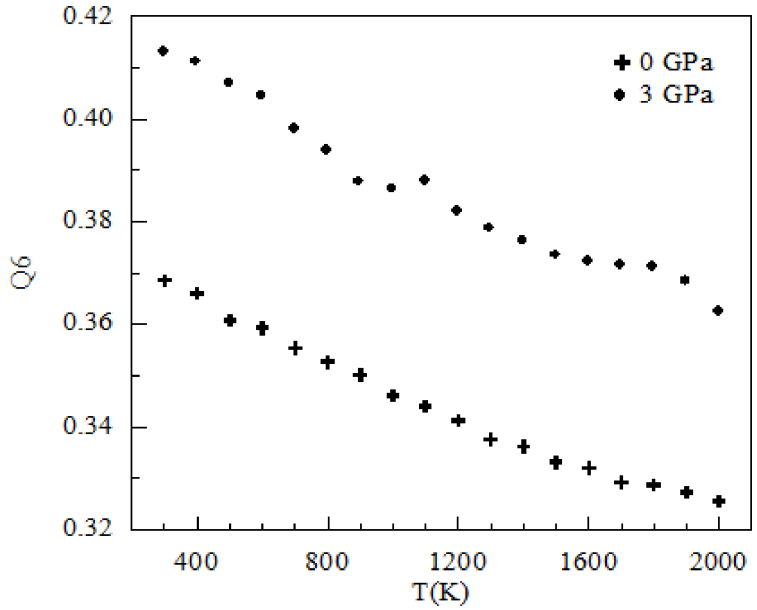

FIG. 10: The value of the bond orientational order parameter under 0 GPa and 3 GPa pressures for the 2×10^{13} K/s cooling rate.

1. For 0, 1, and 3 GPa pressure values, the PdAg binary model alloy system shows a crystal structure at cooling rates of 2×10^{11} and 2×10^{12} K/s. However, the model system is an amorphous structure at 2×10^{13} K/s for all pressure values.

2. The liquid-crystal and liquid-amorphous phase transition temperatures are strongly dependent on the applied pressure. An increase of pressure increases both the crystal forming temperature and the glass transition temperature.

References

[1] H. I. Guntherodt and H. Beck, *Glassy Metals I* (Springer, New York, 1981), Chap. 1.
[2] H. I. Guntherodt and H. Beck, *Glassy Metals III* (Springer, Heidelberg, 1994) Chap. 2.
[3] A. Inoue, Acta Mater. **48**, 279 (2000). doi: 10.1016/S1359-6454(99)00300-6
[4] J. F. Löffler, Intermetallics **11**, 529 (2003). doi: 10.1016/S0966-9795(03)00046-3
[5] P. S. Steif, F. Spaepen, and J. W. Hutchinson, Acta Metall. **30**, 447 (1982). doi: 10.1016/0001-6160(82)90225-5
[6] J. S. Park *et al.*, J. Non-Cryst. Solids **51**, 2142 (2005).
[7] R. D. S. Lisboa and C. S. Kiminami, J. Non-Cryst. Solids **304**, 36 (2002). doi: 10.1016/S0022-3093(02)01001-3
[8] Z. X. Wang, R. J. Wang, and W. H. Wang, Mater. Lett. **60**, 831 (2005).
[9] H. Li, X. Bian, and J. Zhang, Mater. Sci. Eng. A **271**, 116 (1999). doi: 10.1016/S0921-5093(99)00182-3
[10] H. R. Cong, X. F. Bian, J. X. Zhang, and H. Li, Mater. Sci. Eng. A **326**, 343 (2002).

[11] M. Verstraete *et al.*, Comp. Mat. Sci. **30**, 34 (2004).
[12] T. Çağın, G. Dereli, M. Uludoğan, and M. Tomak, Phys. Rev. B **59**, 3468 (1999). doi: 10.1103/PhysRevB.59.3468
[13] R. A. Johnson, Phys. Rev. B **39**, 12554 (1989). doi: 10.1103/PhysRevB.39.12554
[14] J. Liu, J. Z. Zhao, and Z. Q. Hu, Comp. Mat. Sci. **37**(3), 234 (2006).
[15] H. Li and F. Pederiva, Chem. Phys. **304**, 261 (2004). doi: 10.1016/j.chemphys.2004.06.066
[16] Z. X. Wang, R. J. Wang, and W. H. Wang, Mater. Lett. **60**, 831 (2005).
[17] F. Shimojo, K. Hoshino, and Y. Zempo, J. Non-Cryst. Solids **312–314**, 388 (2002).
[18] L. A. Marqués, L. Pelaz, M. Aboy, and P. Lopez, J. Barbolla, Comput. Mater. Sci. **33**, 92 (2005).
[19] Y. Shao, P. C. Clapp, and J. A. Rifkin, Metall. Mater. Trans. A **27A**, 1477 (1996).
[20] M. S. Daw and R. D. Hatcher, Solid State Comm. **56**, 697 (1985). doi: 10.1016/0038-1098(85)90781-1
[21] A. F. Voter and S. P. Chen, Mat. Res. Soc. Symp. Proc. **82**, 175 (1987).
[22] M. W. Finnis and J. E. Sinclair, Philos. Mag. **50**, 45 (1984). doi: 10.1080/01418618408244210
[23] A. P. Sutton and J. Chen, J. Phil. Mag. Lett. **61**, 139 (1990). doi: 10.1080/09500839008206493
[24] M. Grujicic and P. Dang, Mater. Sci. Eng. A **201**, 194 (1995). doi: 10.1016/0921-5093(94)09735-6
[25] J. Gui *et al.*, J. Phys.: Condens. Matter **6**, 4601 (1994). doi: 10.1088/0953-8984/6/24/019
[26] D. Caprion and H. R. Schober, J. Non-Cryst. Solids **326**, 369 (2003). doi: 10.1016/S0022-3093(03)00437-X
[27] H. H. Kart, M. Tomak, M. Uludoğan, and T. Çağın, Comp. Mater. Sci. **32**, 107 (2005).
[28] J. M. Haile, *Molecular Dynamics Simulation, Elementary Methods* (John Wiley & Sons, Inc., Mississauga, 1992), Chap. 2.
[29] D. R. Nelson, Phys. Rev. B **28**, 5515 (1983). doi: 10.1103/PhysRevB.28.5515
[30] P. J. Steinhardt, R. Nelson, and M. Ronchetti, Phys. Rev. B **28**, 784 (1983). doi: 10.1103/PhysRevB.28.784
[31] T. Aste, M. Saadatfar, and T. J. Senden, Phys. Rev. E **71**, 061302 (2005). doi: 10.1103/PhysRevE.71.061302
[32] J. S. Van Duijneveldt and D. Frenkel, J. Chem. Phys. **96**, 4655 (1992). doi: 10.1063/1.462802
[33] D. Caprion and H. R. Schober, J. Non-Cryst. Solids **326–327**, 369 (2003). doi: 10.1016/S0022-3093(03)00437-X
[34] L. Wang, C. Peng, Y. Wang, and Y. Zhang, Phys. Lett. A **350**, 69 (2006).
[35] M. Shimono and H. Onodera, Mat. Sci. Eng. A **304–306**, 515 (2001).
[36] L. Kurmanaeva, *Design and Mechanical Performance of Fully Dense Nanocrystalline Noble Metals on the Basis of Pd, Pd-Ag and Pd-Au*, Ph.D. Thesis (der Fakultät für Ingenieurwissenschaften und Informatik der Universität Ulm, 2011).
[37] M. D. Rintoul and S. Torquato, J. Chem. Phys. **105**, 9258 (1996). doi: 10.1063/1.473004
[38] L. Qi, H. F. Zhang, and Z. Q. Hu, Intermetallics **12**, 1191 (2004). doi: 10.1016/j.intermet.2004.04.003
[39] S. Özdemir Kart, M. Tomak, M. Uludoğan, and T. Çağın, Mat. Sci. Eng. A **435–436**, 737 (2006). doi: 10.1016/j.msea.2006.07.120
[40] M. R. Hoare and N. Y. Ann, Acad. Sci. **279**, (1976). doi: 10.1111/j.1749-6632.1976.tb39707.x
[41] H. Li and F. Pederiva, Chem. Phys. **304**, 261 (2004). doi: 10.1016/j.chemphys.2004.06.066
[42] T. Zhang, T. Gu, and X. Zhang, Model. Simul. Mater. Eng. **13**, 753 (2005). doi: 10.1088/0965-0393/13/5/008